

SOME DESIGN EXPERIMENTS  
TOWARD AN OPERATIONAL  
PRIMITIVE-EQUATION MODEL  
FOR THE TROPICS

CHARLES GEORGE STEINBRUCK

LIBRARY  
VAL POSTGRADUATE S  
ONTEREY, CALIF. 939









RY  
POSTGRADUATE S  
CALIF. ST

# United States Naval Postgraduate School



## THE SIS

SOME DESIGN EXPERIMENTS TOWARD AN OPERATIONAL  
PRIMITIVE-EQUATION MODEL FOR THE TROPICS

by

Charles George Steinbruck

Thesis Advisor:

R. L. Elsberry

September 1971

*Approved for public release; distribution unlimited.*





Some Design Experiments Toward an Operational  
Primitive-Equation Model for the Tropics

by

Charles George Steinbruck  
Lieutenant Commander, United States Navy  
B.S., New York University, 1961

Submitted in partial fulfillment of the  
requirements for the degree of

MASTER OF SCIENCE IN METEOROLOGY

from the

NAVAL POSTGRADUATE SCHOOL  
September 1971



## ABSTRACT

A barotropic and two- and three-layer baroclinic primitive equation prediction models are developed from a ten-layer model previously designed for short range forecasts in the tropics. Twenty-four hour predictions from the models are compared to evaluate any degradation in the forecasts as the vertical resolution of the models decreases. The barotropic primitive equation model on a global tropical grid is used to evaluate the possibility of using a numerical variational analysis as an initialization technique. Initialization of data with the nonlinear balance equation is used as a comparison.



TABLE OF CONTENTS

I.	INTRODUCTION - - - - -	8
II.	PRIMITIVE EQUATION PREDICTION MODEL - - - - -	10
	A. BASIC MODEL - - - - -	10
	B. BAROTROPIC ONE-LAYER MODEL - - - - -	12
	C. BAROCLINIC TWO-LAYER MODEL - - - - -	13
	D. BAROCLINIC THREE-LAYER MODEL - - - - -	15
	E. BOUNDARY CONDITIONS - - - - -	15
	1. No-Flux Boundaries - - - - -	16
	2. Restoration or Constant-Flux Boundaries -	16
	3. Interpolated Boundary Conditions - - - -	17
III.	DATA INITIALIZATION - - - - -	18
	A. NONLINEAR BALANCE EQUATION - - - - -	19
	B. NUMERICAL VARIATIONAL ANALYSIS - - - - -	20
IV.	RESULTS - - - - -	22
	A. PREDICTION EXPERIMENTS WITH THE LIMITED GRID	22
	1. Barotropic Model - - - - -	22
	2. Two-Layer Model - - - - -	23
	3. Three-Layer Model - - - - -	23
	B. EXPERIMENTS ON THE GLOBAL BAND - - - - -	24
V.	CONCLUSIONS AND RECOMMENDATIONS - - - - -	29
	BIBLIOGRAPHY - - - - -	50
	INITIAL DISTRIBUTION LIST - - - - -	52
	FORM DD 1473 - - - - -	54



## LIST OF ILLUSTRATIONS

- Fig. 1. Vertical distribution of variables in the ten-layer model.
- Fig. 2. Vertical distribution of variables in the barotropic model.
- Fig. 3. Vertical distribution of variables in the two-layer model.
- Fig. 4. Vertical distribution of variables in the three-layer model.
- Fig. 5. Limited grid. There are 510 computational points. The grid spacing of 1.5 degrees longitude at 22.5N is shown in the upper left corner.
- Fig. 6. FNWC Monterey Tropical Global Mercator Projection. There are 7105 computational points with grid spacing of 2.5 degrees longitude at the equator.
- Fig. 7. Restoration coefficients near the northern boundary of the tropical global belt. A persistence forecast results at the boundary, a fully dynamic forecast seven rows in, and a blend in-between.
- Fig. 8. Twenty-four hour 250 mb height forecast from the barotropic model.
- Fig. 9. Twenty-four hour 250 mb height forecast from the ten-layer model.
- Fig. 10. Total (T), zonal (Z), and eddy (E) kinetic energies vs. time for the barotropic model on the limited grid.
- Fig. 11. Total (T), zonal (Z), and eddy (E) kinetic energies vs. time for the two-layer model on the limited grid. Solid lines indicate 250 mb data while dashed lines indicate 450 mb data.
- Fig. 12. Twenty-four hour 250 mb height forecast from the three-layer model.





- Fig. 13. Twenty-four hour 750 mb height forecast from the three-layer model.
- Fig. 14. Twenty-four hour 750 mb height forecast from the ten-layer model.
- Fig. 15. Twenty-four hour 1000 mb height forecast from the three-layer model.
- Fig. 16. Twenty-four hour 1000 mb height forecast from the ten-layer model.
- Fig. 17. Initialization of the 500 mb height field by the nonlinear balance equation technique. Solid lines are initial data while dashed lines are the departure from the 500 mb climatology used as input.
- Fig. 18. Initialization of the 500 mb height field by the numerical variational analysis technique. Solid lines are initial data while dashed lines are the departure from the 500 mb climatology used as input.
- Fig. 19. Twenty-four hour 250 mb height forecast from the barotropic model on the global grid with restoration boundary conditions and numerical variational analysis initialization.
- Fig. 20. Twenty-four hour 250 mb height forecast from the barotropic model on the global grid with no-flux boundary conditions and nonlinear balance equation initialization.
- Fig. 21. Total (T), zonal (Z), and eddy (E) kinetic energies vs. time for the barotropic model on the global grid. Solid lines are for the basic model while dashed lines are for the model with diffusion terms included.
- Fig. 22. Twenty-four hour 250 mb height forecast from the barotropic model with diffusion terms, restoration boundary conditions and numerical variational analysis initialization.



# LIST OF SYMBOLS

$C_d$	Drag coefficient
$C_p$	Specific heat of air at constant pressure
$f$	Coriolis parameter
$F_x, F_y$	Frictional terms of momentum equations
$g$	Acceleration of gravity
$I$	Grid index in x (east-west) direction
$J$	Grid index in y (north-south) direction
$K$	Grid index in vertical (pressure) direction
$m$	Map factor
$P$	Pressure (independent variable)
$R$	Gas constant
$q$	Specific humidity
$t$	Time (independent variable)
$u$	Velocity component in x direction
$v$	Velocity component in y direction
$x, y$	Independent variables (east-west, north-south)
$Z$	Height of constant pressure surface
$\rho$	Density of air
$\tau_x, \tau_y$	Frictional surface stress
$\phi$	Geopotential height
$\omega$	Velocity component in vertical (pressure) direction
$\theta$	Potential temperature



## ACKNOWLEDGEMENT

The author wishes to express his sincere appreciation to Professor R. L. Elsberry for the support and guidance he patiently provided during this research.

The author is also indebted to Dr. J. M. Lewis, who gave generously of his time and talents in the adaption of the numerical variational analysis technique to the prediction model.

Finally, the author wishes to express his thanks to Captain W. S. Houston, Jr. and the personnel of Fleet Numerical Weather Central, Monterey, for the computer support provided.



## I. INTRODUCTION

Weather prediction in the tropics has always suffered, basically from a paucity of data. Hemispheric numerical prediction models not only suffer from this deficiency, but setting the boundary conditions in the tropics probably also deteriorates the product in this area.

In recent years there has been some increase in meteorological data over the tropical regions, particularly in the form of commercial aircraft reports. This increase allowed Fleet Numerical Weather Central, Monterey, to commence an objective analysis for a global belt centered in the tropics. In addition, FNWC was also investigating the use of a numerical variational analysis scheme for this global belt. Since this scheme simultaneously solved for the wind and mass fields using the maximum amount of data, it could potentially be used as an initial state for a tropical numerical prediction model, if the fields were dynamically consistent.

Multi-layer baroclinic numerical primitive equation prediction models for limited regions in the tropics have been developed by Krishnamurti (1969), Miller (1969), Harrison (1969), and Elsberry and Harrison (1971). Vanderman and Collins (1967) have used a barotropic primitive equation model for operational experiments with data from a global tropical belt.





The availability of tropical data for a global belt, along with the limited-region prediction model developed by Elsberry and Harrison provided the impetus for this work. The object of this thesis then, is to perform experiments involving the initialization of data and the development of a primitive equation model for short range tropical forecasts on an operational basis.



## II. PRIMITIVE EQUATION PREDICTION MODEL

### A. BASIC MODEL

A ten-layer primitive equation model, developed by Harrison (1969) and Elsberry and Harrison (1970, 1971), was used to formulate less complex models for possible operational use. The original model was developed for short range predictions over a 34x15 point tropical grid, with a grid distance of 1.5 degrees longitude at 22.5 N. A frictionless, adiabatic version of this model required approximately 20 minutes of computer time to produce a twenty-four hour prognosis.

The equations for the ten-layer model are as follows:

$$\frac{\partial u}{\partial t} = -L(u) + fv - m \frac{\partial \phi}{\partial x} + F_x \quad (1)$$

$$\frac{\partial v}{\partial t} = -L(v) - fu - m \frac{\partial \phi}{\partial y} + F_y \quad (2)$$

$$\frac{\partial \theta}{\partial t} = -L(\theta) + \text{HEAT} \quad (3)$$

$$\frac{\partial q}{\partial t} = -L(q) + \text{MOISTURE} \quad (4)$$

$$\frac{\partial \phi_{1000}}{\partial t} = -L(\phi_{1000}) \quad (5)$$

$$\frac{\partial \omega}{\partial p} = -m^2 \left[ \frac{\partial}{\partial x} \left( \frac{u}{m} \right) + \frac{\partial}{\partial y} \left( \frac{v}{m} \right) \right] \quad (6)$$

$$\Delta \phi = \hat{\theta} c_p \Delta \left( \frac{p}{1000} \right)^{R/c_p} \quad (7)$$

$$\text{where} \quad L(s) = m^2 \left[ \frac{\partial}{\partial x} \left( \frac{su}{m} \right) + \frac{\partial}{\partial y} \left( \frac{sv}{m} \right) \right] + \frac{\partial}{\partial p}(\omega s) \quad (8)$$



The ten-layer model averaged parameters over two points only, in the direction of the space derivative. Finite differencing on a constant pressure surface, for the general variable S is as follows:

$$\frac{\partial}{\partial y} \left( \frac{Sv}{m} \right) = \left\{ \left[ S(I, J+\frac{1}{2}, K) \right] \frac{1}{2} \left[ \frac{v(I, J+1, K)}{m(J+1)} + \frac{v(I, J+1, K)}{m(J)} \right] - \left[ S(I, J-\frac{1}{2}, K) \right] \frac{1}{2} \left[ \frac{v(I, J, K)}{m(J)} + \frac{v(I, J-1, K)}{m(J-1)} \right] \right\} \frac{1}{\Delta y}$$

where

$$S(I, J+\frac{1}{2}, K) = \frac{S(I, J+1, K) + S(I, J, K)}{2} ,$$

$$S(I, J-\frac{1}{2}, K) = \frac{S(I, J-1, K) + S(I, J, K)}{2} .$$

An important feature of the model is the vertical distribution of variables, as shown in Fig. 1, since vertical motion is not averaged. All other parameters are averaged uniformly in the vertical, except at the lowest level. Vertical differencing is as follows:

$$\frac{\partial}{\partial p} (\omega_s) = \left\{ \left[ \omega(I, J, K+1) \right] \left[ S(I, J, K+1) \right] - \left[ \omega(I, J, K-1) \right] \left[ S(I, J, K-1) \right] \right\} \frac{1}{\Delta p} ,$$

where

$$S(I, J, K+1) = \frac{S(I, J, K+2) + S(I, J, K)}{2} ,$$

$$S(I, J, K-1) = \frac{S(I, J, K) + S(I, J, K-2)}{2} .$$



Arakawa (1966) showed this finite difference flux form conserves the mean square of potential temperature and mean square kinetic energy while preventing nonlinear instability caused by aliasing. The model remained computationally stable with minimal smoothing or averaging utilizing a six-minute time step.

The first time step is forward, where for the general parameter  $S$ , time step,  $n$ , and time difference,  $\Delta t$ ,

$$S^{n+1} = S^{n=0} + \Delta t f(S^{n=0})$$

Centered or leapfrog time steps are used for subsequent time steps, where

$$S^{n+1} = S^{n-1} + 2\Delta t f(S^n).$$

Reinitialization, to avoid solution separation, during the twenty-four hour period was not found to be necessary.

## B. BAROTROPIC ONE-LAYER MODEL

Modification of the ten-layer model into a one-layer barotropic model was the first step in the development of an operational model. The 250 mb surface was chosen as the optimum forecast level due to the relatively high density of observations in the tropics at this level, according to Krishnamurti (1970).

Vertical distribution of variables in the one-layer barotropic model is shown in Fig. 2. Required inputs are the winds and geopotential at 250 mb. A fictitious 1000 mb geopotential is derived, utilizing the barotropic assumption, to maintain a similarity between the barotropic one-layer





and the ten-layer model. Since this is a barotropic model Equations (3) and (4) are not required. In addition, the frictional terms in Equations (1) and (2) are neglected.

Initial experiments were conducted using the 510 point grid that was used in the development of the ten-layer model. This grid is illustrated in Fig. 5. Approximately two minutes of computer time is required for a twenty-four hour prognosis.

Later work was performed using the FNWC (Monterey) Tropical Global Mercator Projection, shown in Fig. 6. This is a 144x49 point grid with a grid distance of 2.5 degrees longitude at the equator. A twenty-four hour barotropic prediction on the global band requires approximately 25 minutes of computer time.

### C. BAROCLINIC TWO-LAYER MODEL

As a second step, a two-layer model of the atmosphere was developed to include the effects of friction in the surface layer. With the exception of Equation (4), the full set of equations was used in this model. However, in addition to not predicting moisture, diabatic heating was neglected so that in Equation (3) only advection was permitted to change the initial temperature field.

The vertical distribution of variables in the two-layer model is shown in Fig. 3. Required inputs are the winds, geopotential, and temperatures at 950 and 250 mb, and the geopotential and temperature at 1000 mb.



The friction terms are given by the bulk aerodynamic transport relations

$$F_x = -g \frac{\partial \gamma_x}{\partial p},$$

$$F_y = -g \frac{\partial \gamma_y}{\partial p},$$

where

$$\gamma_x = g C_d |V| u,$$

$$\gamma_y = g C_d |V| v.$$

The values of the drag coefficient,  $C_d$ , are

$$C_d = 0.5 |V|^{\frac{1}{2}} \times 10^{-3},$$

for winds from 1 to 15 meters per second, and

$$C_d = 2.6 \times 10^{-3},$$

for wind speeds greater than 15 meters per second. The wind used in the above calculation is a linear function of the 950 mb wind with the direction held constant and the speed reduced 20 %. Friction is considered only in the layer between 1000 and 900 mb, where the stress and the vertical gradient of stress are both assumed to be zero at 900 mb.

As stated earlier, the upper level of most interest was the 250 mb level. However, this implies that the wind field in the very deep upper layer is defined by a level near the upper extreme of the layer. Consequently, the two layer baroclinic model was also tested in experiments with the 350, 450, or 550 mb level replacing 250 mb as the upper wind level.



All experiments with the two-layer model were conducted using the 510 point grid. A twenty-four hour prognosis required approximately seven minutes of computer time.

#### D. BAROCLINIC THREE-LAYER MODEL

Inclusion of data at the 750 mb level produced a three-layer version of the baroclinic model to provide a more realistic approximation of the atmosphere. The 800 mb above the surface layer was divided into two layers at the 500 mb level. The development of this model also presented the opportunity to evaluate the effect of increased vertical resolution versus the resulting increase in computer storage and time requirements. Fig. 4 illustrates the vertical distribution of variables for the baroclinic three-layer model.

All experiments with this model were conducted with the 510 point grid. Computer time of approximately nine minutes is required for a twenty-four hour prediction.

#### E. BOUNDARY CONDITIONS

The computationally stable integration of the primitive equations requires a set of boundary conditions that are consistent with the finite difference scheme.

Flux through the top of the domain is eliminated by setting  $\omega = 0$ .

At the lowest level, 1000 mb, Equation (5) is imposed.

Experiments were conducted with three sets of horizontal boundary conditions.



## 1. No-flux boundaries

Elsberry and Harrison (1971) discuss the boundary conditions which are applicable to the basic model. Initialization was accomplished using the nonlinear balance equation after computing the rotational component of the wind.

The requirement for east-west boundary conditions on the 510 point grid is eliminated by making the data cyclical in the initialization. Naturally, east-west boundary conditions are not necessary on the global band.

By setting

$$v_{j+1} = - \frac{m_{j+1}}{m_j} v_j, \quad u_{j+1} = u_j, \quad \text{and} \quad \phi_{j+1} = \phi_j,$$

where  $j+1$  is the northern-most row in the grid, no flux of mass or energy is allowed. The southern boundary is treated in a similar manner.

## 2. Restoration or constant-flux boundaries

Kesel and Winninghoff (1970) describe a constant-flux, restoration boundary technique that eliminates both the necessity for altering the initial mass structure and the false reflection of the computational mode at the boundary. Initial height and wind fields near the boundaries are preserved. At the completion of each time step the newly predicted values of the fields are restored toward values at the previous time step with a specified field of restoration coefficients. Figure (7) illustrates the restoration field near the northern boundary. The procedure





results in a fully dynamic forecast seven rows in from the boundary, a persistence forecast for the two rows at the boundary, and a blend in-between. Restoration boundary conditions were restricted to experiments using the global grid.

### 3. Interpolated boundary conditions

Krishnamurti (1969) used implicit north and south poles to define boundary values. Geopotential values at the north pole are defined by the mean value at row  $j$ , where the north boundary is row  $j+1$ . The three components of the wind are assumed to be zero at the pole. A linear interpolation between the pole and row  $j$  is performed each time step to calculate the values of the four parameters at row  $j+1$ . A similar calculation specifies the southern boundary. Experiments with interpolated boundary conditions were confined to the global band.



### III. DATA INITIALIZATION

The importance of initial conditions for a primitive equation model has long been recognized. Raw meteorological data, used as an input, quickly results in high frequency inertio-gravity oscillations. Shuman and Hovermale (1969), Benwell and Bretherton (1968), Smagorinsky et al. (1965), Charney (1955), and Hinkelmann (1951) all propose an initial state with no divergence or vertical motion, to suppress these oscillations. Phillips (1960), however, showed that for a simple linear model an initial divergence equal to that suggested by quasi-geostrophic balance is required. Hinkelmann (1959) demonstrated that high frequency oscillations will be filtered out if the time derivative of divergence vanishes in the initial field, that is if

$$\frac{\partial^n D}{\partial t^n} = 0 \quad (9)$$

where  $D$  is the divergence and  $n=1,2,3,\dots$ . Note that using the balance equation to specify the initial conditions results in satisfying the above conditions for  $n=1$ . Finally, this condition has been satisfied for  $n=1$  and  $2$  by Miyakoda and Moyer (1968) and Nitta and Hovermale (1969), by integrating the primitive equations forward and backward until the initial field meets the condition. Two types of initialization were tested in this series of experiments.



## A. NONLINEAR BALANCE EQUATION

Elsberry (1969) utilized the nonlinear balance equation and special boundary conditions to formulate a diagnostic model that would match the prognostic model (ten-layer with no-flux boundary conditions). The nondivergent part of the wind was obtained from

$$\nabla^2 \psi = \zeta,$$

where  $\zeta$  is the relative vorticity from the observed wind components  $u$  and  $v$ . Smoothing the relative vorticity fields in the vertical improved the vertical consistency of the stream-function fields. No normal component of the wind was allowed at the north and south boundaries, implying that these boundaries were streamlines. Thus  $\psi_n$  and  $\psi_s$  were set equal to constants at each of the boundaries with

$$\psi_n - \psi_s = \bar{u} \Delta y,$$

where  $\bar{u}$  is the mean zonal wind component averaged over the grid, and  $\Delta y$  is the distance between the north and south boundaries. In the manner of Krishnamurti (1969) the grid was extended by five points between the east and west ends of the grid which are linearly matched, providing cyclical continuity.

The  $\psi$  field was used to determine the geopotential from the nonlinear balance equation,

$$\nabla^2 \phi = \nabla \cdot f \nabla \psi + 2J \left( \frac{\partial \psi}{\partial x}, \frac{\partial \psi}{\partial y} \right)$$

Boundary conditions on  $\phi$  at the northern and southern walls were made geostrophically consistent with the streamfunction



difference ( $\Psi_n - \Psi_s$ ) by using a mean value of  $f$  across the limited region grid. On the global belt the averages of the observed geopotential heights along the walls were used for the boundary conditions.

## B. NUMERICAL VARIATIONAL ANALYSIS

Sasaki (1958) introduced the variational method to obtain dynamically consistent initial fields, showing theoretically that quasi-geostrophically balanced or divergence-free fields could be obtained as a solution to the Euler-Lagrange equations. Filtering high frequency oscillations using Equation (9) as a low pass filter, where  $D$  is not limited to divergence, but may be any meteorological parameter to be filtered, was also proposed by Sasaki (1970). Long wave equations are used with quasi-steady state conditions as a dynamical constraint in a numerical variational analysis. This method, as adapted by Lewis (1971) for operational use by FNWC, Monterey, was tested as an initialization scheme for the barotropic prediction experiments on the global grid.

The variational analysis was obtained by minimizing the functional

$$J = \iint_S \left\{ \alpha [(u - \tilde{u})^2 + (v - \tilde{v})^2] + \beta (z - \tilde{z})^2 + \alpha \left( \frac{\partial u}{\partial t} \right)^2 + \alpha \left( \frac{\partial v}{\partial t} \right)^2 \right\} dS$$

where the integration is over the surface  $S$  being analyzed. Here  $\tilde{u}$ ,  $\tilde{v}$ , and  $\tilde{z}$  are the observations interpolated to grid-points by an objective analysis scheme, and  $u$ ,  $v$ , and  $z$  are the desired fields which result from the minimization





of  $J$ .  $\tilde{\alpha}$  and  $\tilde{\beta}$  are weighting functions dictated by the density and reliability of observations. The last two terms in the functional can be interpreted as a control on the amount of acceleration in the analysis, and are related to the low pass filter characteristic mentioned earlier. The larger the ratio of the dynamical weight  $\alpha$  to the observational weights,  $\tilde{\alpha}$  and  $\tilde{\beta}$ , the more the analysis will be forced toward a steady state where

$$\frac{\partial u}{\partial t} = -\frac{1}{f} \frac{\partial Z}{\partial x} - \mathbf{v} \cdot \nabla u + fv = 0$$

and

$$\frac{\partial v}{\partial t} = -\frac{1}{f} \frac{\partial Z}{\partial y} - \mathbf{u} \cdot \nabla v - fu = 0.$$

Steady state can only be attained in the limit, if  $\tilde{\alpha}/\alpha$  and  $\tilde{\beta}/\alpha$  are zero over the whole field. The inclusion of some small tendencies in the fields however, may be desirable for the initialization of a primitive equation prediction model.

To enhance the operational value of the variational analysis scheme, Lewis (1971) developed a technique to avoid solving the three equations for the  $u$ ,  $v$ , and  $z$  fields simultaneously. However, this technique involved grouping the inertial terms with the local change terms, and minimizing the imbalance between the remaining terms, the pressure gradient and coriolis terms. The usefulness of the variational analysis for initialization was degraded by this technique, particularly in high wind regions. The technique was then modified to include an approximation of the inertial terms, by evaluating them using the input fields,  $\tilde{u}$  and  $\tilde{v}$ .



## IV. RESULTS

### A. PREDICTION EXPERIMENTS WITH THE LIMITED GRID

This group of experiments is an attempt to test how much a barotropic model and simple baroclinic models degrade the results of the ten-layer model. Data initialization was accomplished using the nonlinear balance equation technique and the prediction models had no-flux boundary conditions. The input data contained both an upper level cold low and the anticyclonic flow over an incipient tropical storm.

#### 1. Barotropic Model

The barotropic model provided a twenty-four hour prognosis that compared very favorably with the twenty-four hour results from the ten-layer model. Figures 8 and 9 illustrate the twenty-four hour prognoses from the respective models. The barotropic prognosis shows essentially the same height pattern as the ten-layer prognosis. The greatest difference is in the height of the cold low, where the barotropic prediction is approximately ten meters higher than the ten-layer prediction.

Figure 10 illustrates the change of the total, zonal, and eddy kinetic energies with respect to time for the barotropic model. Although an apparently spurious increase in the eddy kinetic energy is noted, no degradation of the twenty-four hour prognosis was noted.



## 2. Two-layer Model

The attempt to predict the 250 mb surface with the two-layer model was not successful. The exponential growth of eddy kinetic energy associated with this failure is shown in Fig. 11, where the solid lines indicate the 250 mb kinetic energies. The dashed lines illustrate the 450 mb kinetic energies. Two-layer models with upper levels of 350 and 550 mb also did not exhibit unreasonable growth of the eddy kinetic energy. This implies that perhaps successful predictions could be carried out when the broad upper layer is defined with data from levels lower than 250 mb, or with input data which has been averaged over several layers.

## 3. Three-layer Model

Twenty-four hour prognoses from the three-layer model were very encouraging. The twenty-four hour 250 mb prognosis, as shown in Fig. 12, is almost identical to the ten-layer prognosis shown in Fig. 9. There are no appreciable differences in the heights. Of course, the three-layer model also provides predictions at 750, 950, and 1000 mb. The 750 mb twenty-four hour prognoses as illustrated in Fig. 13 and 14 also have no significant differences. Fig. 15, the three-layer 1000 mb twenty-four hour prognosis, while having the same pattern as Fig. 16, the ten-layer version, has filled the tropical cyclone approximately ten meters more, thus reducing the gradient surrounding the storm.



Thus a three-layer model which would incorporate both the boundary layer and the upper tropospheric flow, which are known to be important in the tropics, may be feasible. The middle layer would be a useful buffer and add an additional degree of freedom for baroclinic development. The scarcity of data in the tropics for this mid-layer could lead to the use of low cloud motions, as measured from the Applied Technology Satellite, for initialization of this level.

Unfortunately, only one data set was available for the experiments with the limited grid and further experiments with more data sets are required before these results may be considered conclusive.

#### B. EXPERIMENTS ON THE GLOBAL BAND

Use of the nonlinear balance equation for the initialization of the primitive equation model has been demonstrated previously by Harrison (1969) and Elsberry and Harrison (1971). Krishnamurti (1969) also used this technique for the initialization of a primitive equation model. The predictions obtained from the barotropic and two- and three-layer models tend to confirm these results. Although only the rotational component of the wind and a smooth height field from the balance equation are used as initial data, a realistic prediction of systems is the resultant.

It was considered sufficient to test the initialization properties of the numerical variational analysis with the







barotropic model in order to save computer time. To assure a good data set, climatological fields were used rather than actual data in the global band experiments. Both 500 mb and 300 mb climatological fields were used. Although only the 500 mb results are discussed and illustrated, the same type problems were encountered with both fields and the solutions were similar. Since the size of the FNWC tropical Mercator projection would not permit a detailed view of the entire grid in this publication, only a small portion of the grid is presented. This portion was chosen as being representative of the problems and solutions encountered with the whole grid and includes the entire north-south extent of the grid, the western Pacific Ocean, the Asian coastline, Japan, Indonesia and Australia. The 500 mb climatological field for January in this area features a broad trough in the north, a band of maximum winds between 30 and 40N, flat high pressure from 20N to 20S and basically zonal flow in the southern hemisphere.

Figure 17 represents the nonlinear balance equation initialization. Solid lines are the initial data while the dashed lines are the departure of the initial data from the 500 mb climatology. Smoothing near the boundaries is apparent as is a large overall height rise caused by the initialization boundary conditions. On a limited tropical grid, setting the heights on the north and south boundaries equal to the mean height is reasonable, however, on the global band, with boundaries well into mid-latitudes, this



is no longer true. In the region of a trough along the boundary, the field will be relaxed toward a boundary that is too high, while the opposite effect will occur in the area where a ridge is along the boundary. New boundary conditions will be required if the nonlinear balance equation initialization technique is to be used on a grid with boundaries in mid-latitudes.

Initial heights as determined by the numerical variational analysis technique are shown in Fig. 18 as solid lines. The dashed lines depict the deviation of the initial heights from the climatological 500 mb data. It is readily apparent that this technique does not significantly alter the input field.

Perhaps the greatest advantage to be realized by using the numerical variational analysis technique for initialization is provided by the opportunity to vary the weighting functions over the analysis. In sparse data regions the dynamical weight,  $\alpha$ , can be increased. In mid-latitudes the height field weight,  $\tilde{\beta}$ , can be increased, while in the tropics the wind field weight,  $\tilde{\alpha}$ , can be increased. The proper utilization of the weighting functions should guarantee a dynamically consistent input for primitive equation models.

To determine if the variational analysis technique would initialize the barotropic model, a twenty-four hour prediction with initialization by this scheme was compared to a similar prediction with initialization by the nonlinear balance equation technique. Restoration boundary conditions



were used in the model with the variational initialization. Figure 19 illustrates the twenty-four hour prediction for this technique. The twenty-four hour prediction for the model initialized with the balance equation is shown in Fig. 20. This model used no-flux boundary conditions. Ignoring the height differences caused by the initialization techniques, and particularly in regions away from the boundaries, the predictions are very similar. Only the developing short wave features in the wind maximum between 30N and 40N are disturbing. In all, three sets of boundary conditions, no-flux, restoration, and interpolated, were tested with the two initialization techniques. All combinations developed the short wave features mentioned above. There were no problems in the predominantly zonal southern hemisphere, nor were there any short period height oscillations at the equator as noted by Winninghoff (1971) and Krishnamurti (personal communication). The conclusion to be drawn from these limited experiments then is that the short wave features are independent of either boundary conditions or initialization and that the variational analysis technique will successfully initialize the barotropic primitive equation prediction model.

The solid curves in Fig. 21 illustrate kinetic energy changes for the restoration-variational analysis prediction model for the forecast period. The growth of kinetic energy is attributed to an accumulation of energy in the smallest permitted scales as the eddy kinetic energy appears to be





the forcing function. This phenomena was also noted by Kesel (1968), in a barotropic primitive equation experiment using a hemispheric grid.

The accumulation of the eddy kinetic energy was controlled by adding a term to the momentum equations to simulate lateral diffusion of momentum, in the form

$$\kappa_m^2 \nabla^2 u \quad \text{and} \quad \kappa_m^2 \nabla^2 v,$$

where  $\kappa$ , the lateral eddy diffusion coefficient is a function of the grid distance.

A twenty-four hour prognosis as obtained from the barotropic model, with lateral diffusion terms included ( $\kappa=5 \times 10^6$ ), restoration boundary conditions and variational analysis initialization is shown in Fig. 22. Note that the aforementioned short-wave features are absent. The dashed lines in Fig. 21 illustrate the kinetic energy changes for the model with the diffusion term included. That the lateral diffusion term prevents accumulation of energy in the small grid scales is evident.





## V. CONCLUSIONS AND RECOMMENDATIONS

A barotropic or three-layer primitive equation prediction model for use in the tropics on an operational basis seems well within reach, whether on a limited region or a global basis. The basic model for use on the FNWC tropical Mercator grid has been tested. Further experiments are required to isolate the cause of and either eliminate or control the accumulation of eddy kinetic energy. As the prediction models become more refined, a staggered grid system should be investigated to further reduce computer time and storage requirements.

The successful use of the nonlinear balance equation for initialization of a limited-region primitive equation prediction model has been demonstrated by Krishnamurti (1969) and Elsberry (1969). However, if this scheme is to be utilized when the boundaries are in areas with height gradients larger than those encountered in the tropics, more suitable boundary conditions must be developed. Over a global band, no-flux boundary conditions may not be crucial and other boundary conditions may be applicable.

The numerical variational analysis technique has been adapted for use in initializing the barotropic primitive equation model. Using the nonlinear balance equation initialization scheme as a comparison, it would appear as if the numerical variational analysis will successfully



initialize a primitive equation prediction model. Further experiments with operational data will be required to determine the optimum values of the weighting functions.



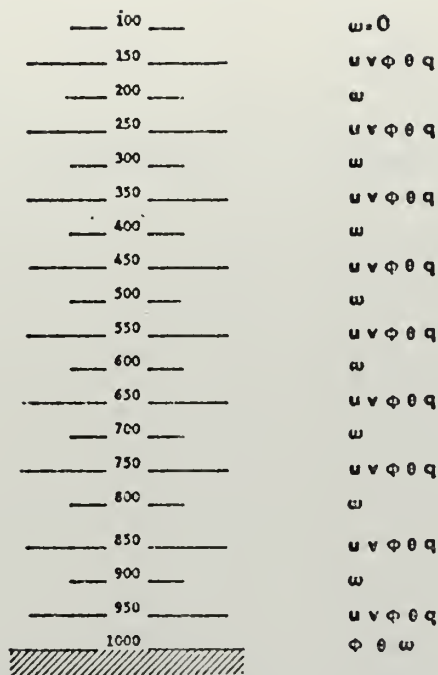


Fig. 1. Vertical distribution of variables in the ten-layer model.



Fig. 2. Vertical distribution of variables in the barotropic model.



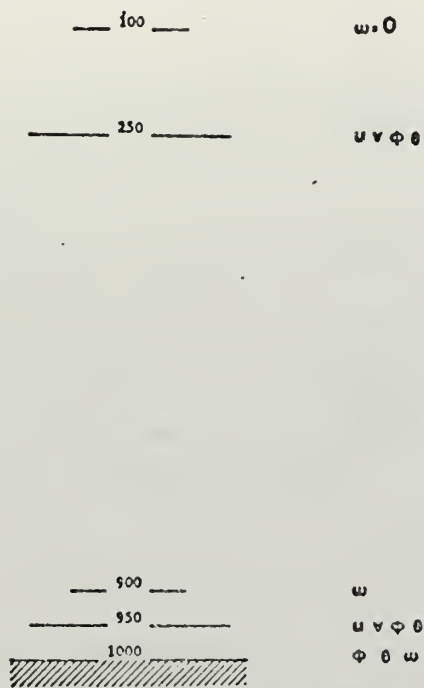


Fig. 3. Vertical distribution of variables in the two-layer model.

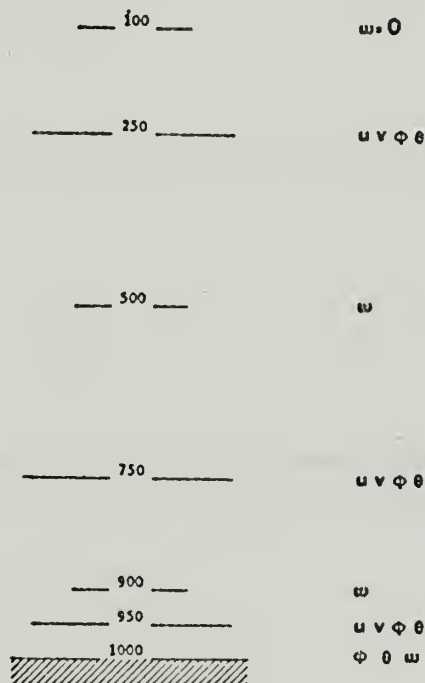


Fig. 4. Vertical distribution of variables in the three-layer model.





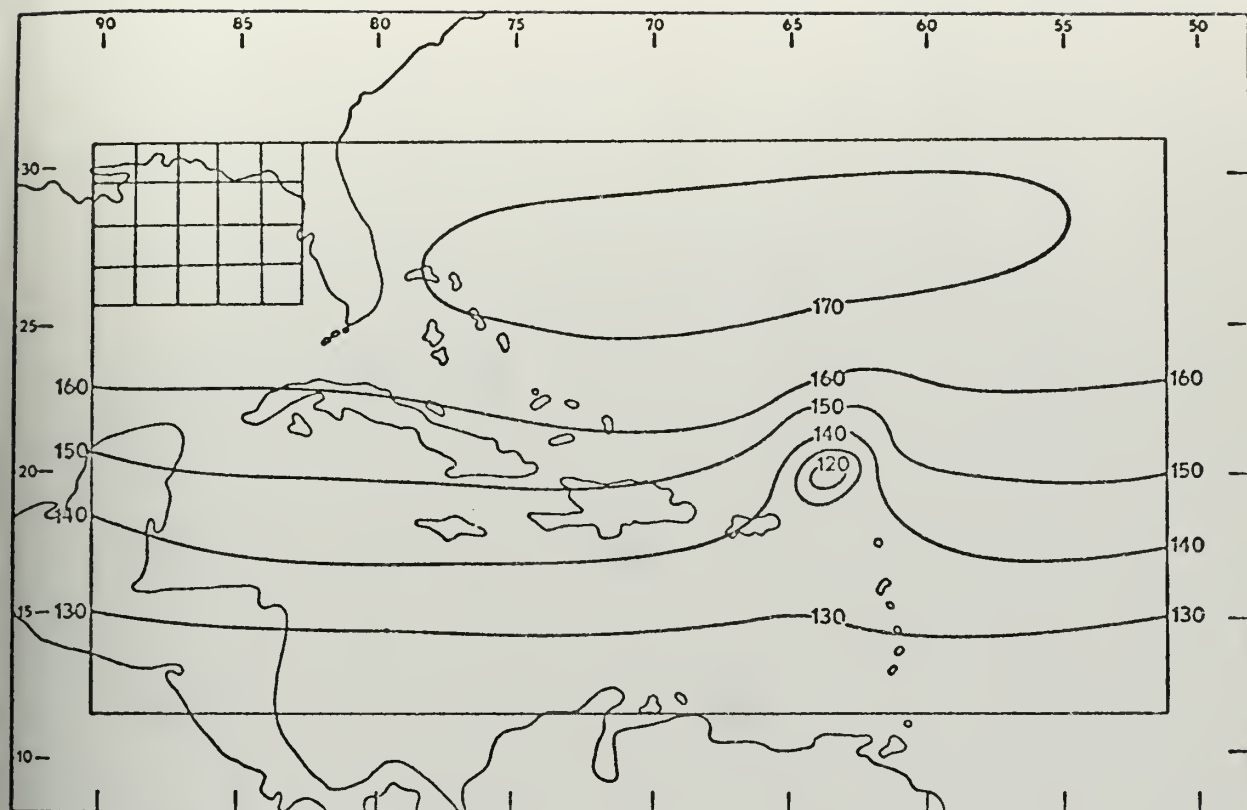


Fig. 5. Limited grid. There are 510 computational points. The grid spacing of 1.5 degrees longitude at 22.5N is shown in the upper left corner.

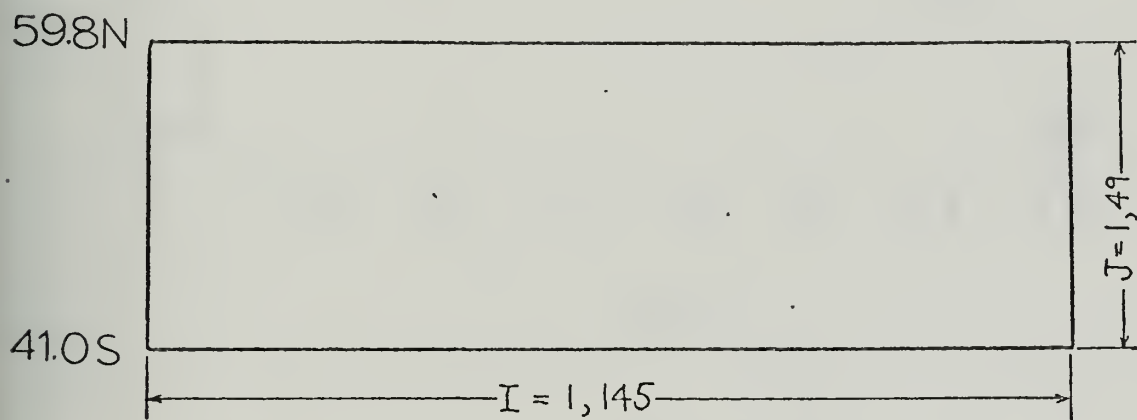


Fig. 6. FNWC, Monterey, Tropical Global Mercator Projection. There are 7105 computational points with grid spacing of 2.5 degrees longitude at the equator.



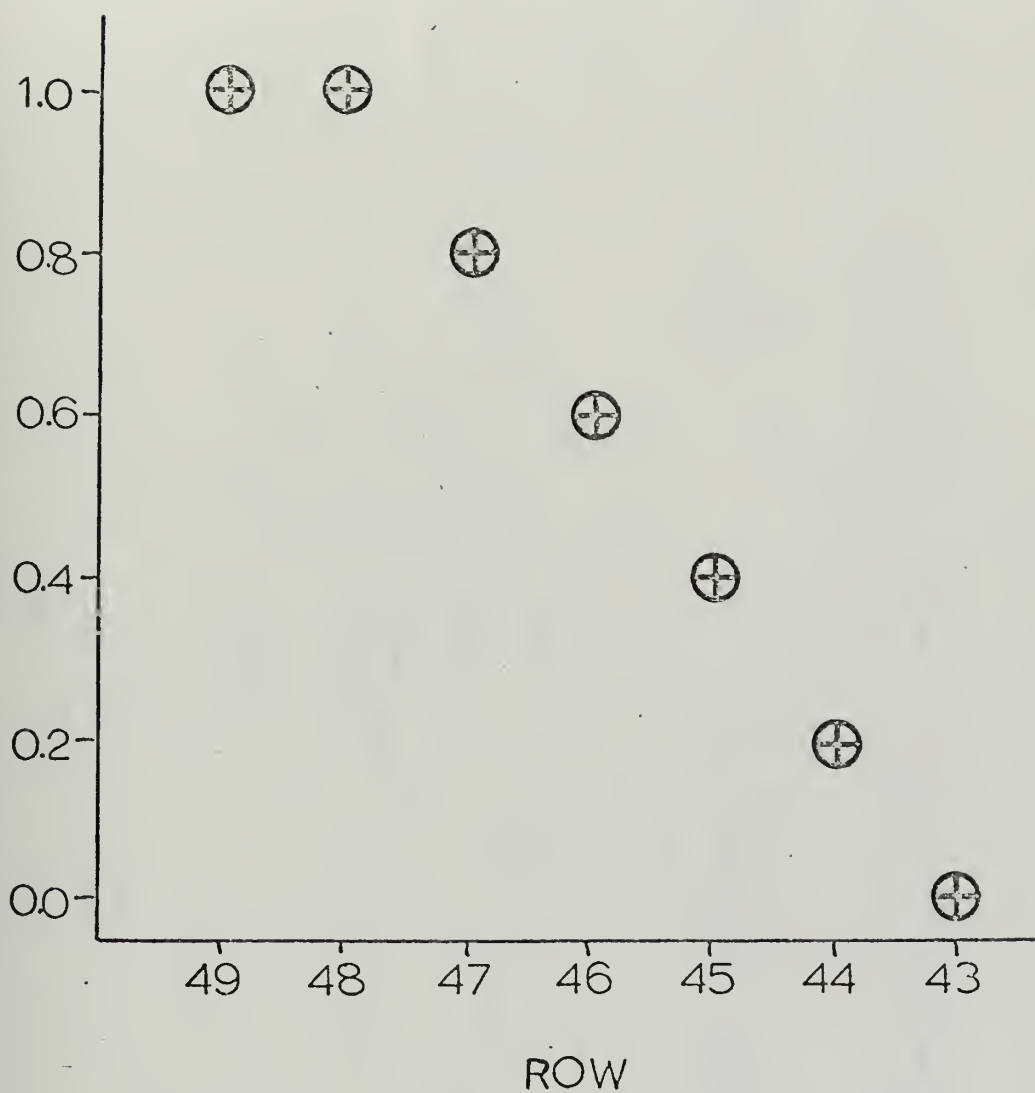


Fig. 7. Restoration coefficients near the northern boundary of the tropical global belt. A persistence forecast results at the boundary, a fully dynamic forecast seven rows in, and a blend in-between.



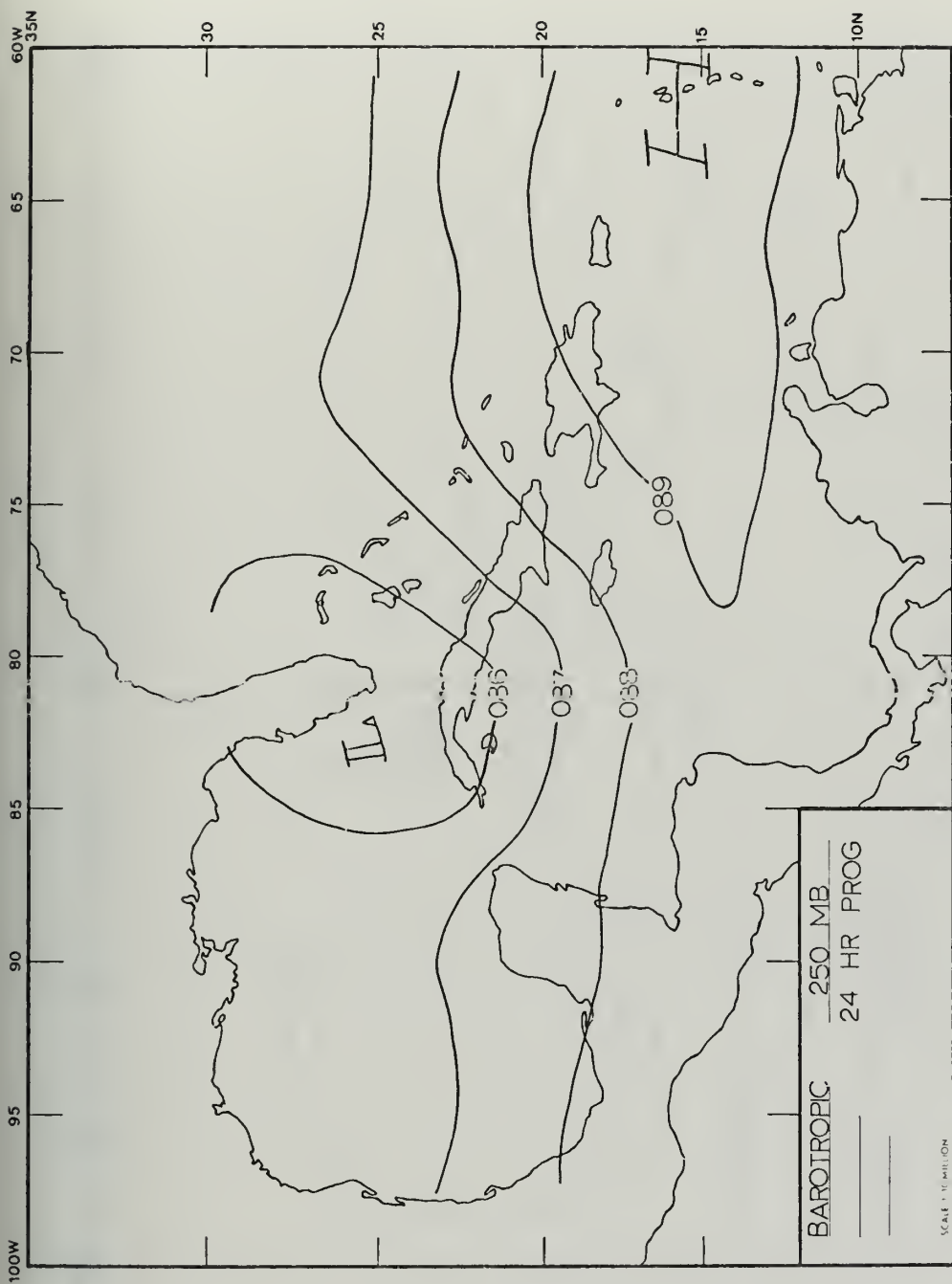


Fig. 8. Twenty-four hour 250 mb height forecast from the barotropic model.



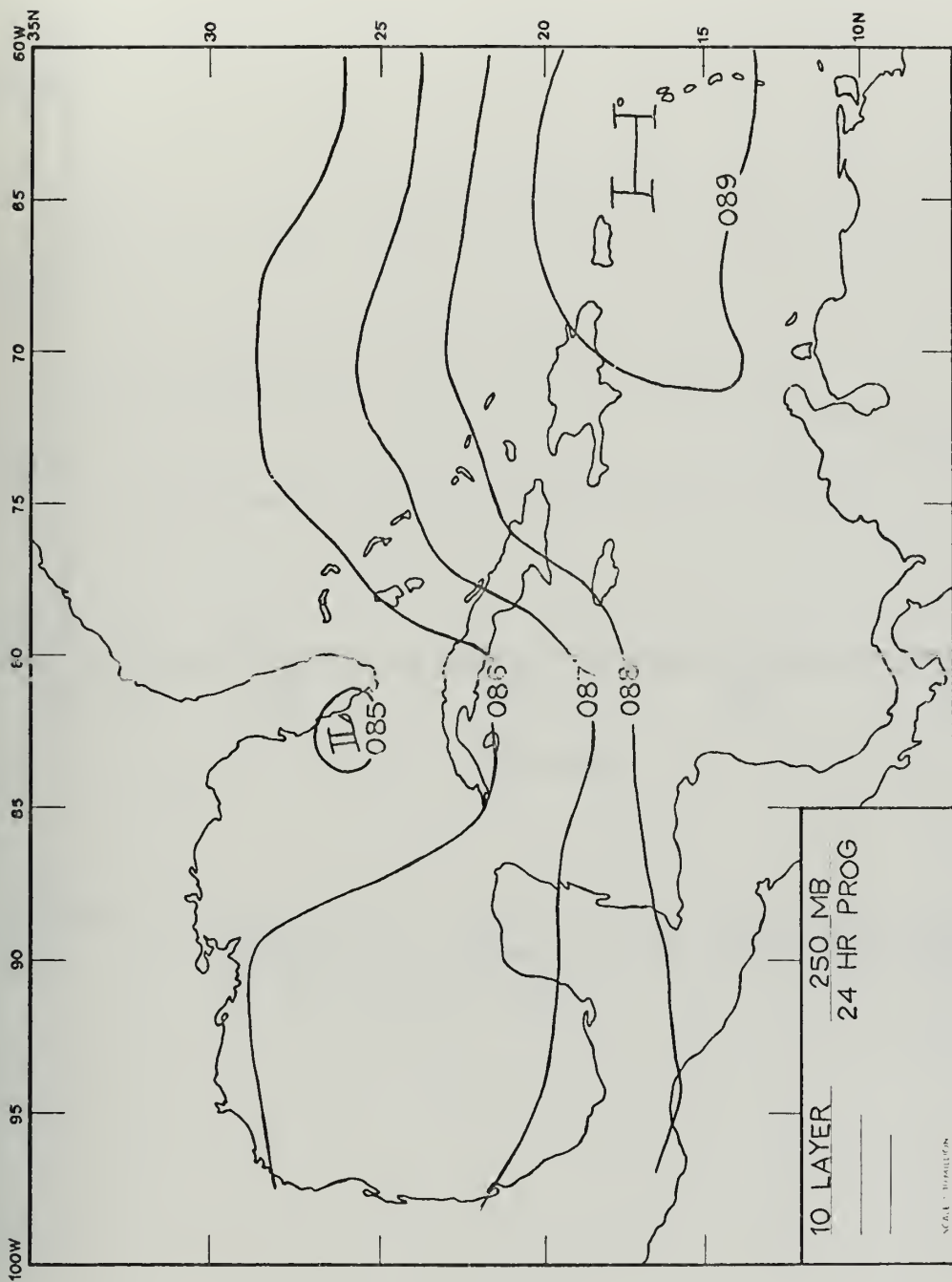


Fig. 9. Twenty-four hour 250 mb height forecast from the ten-layer model.





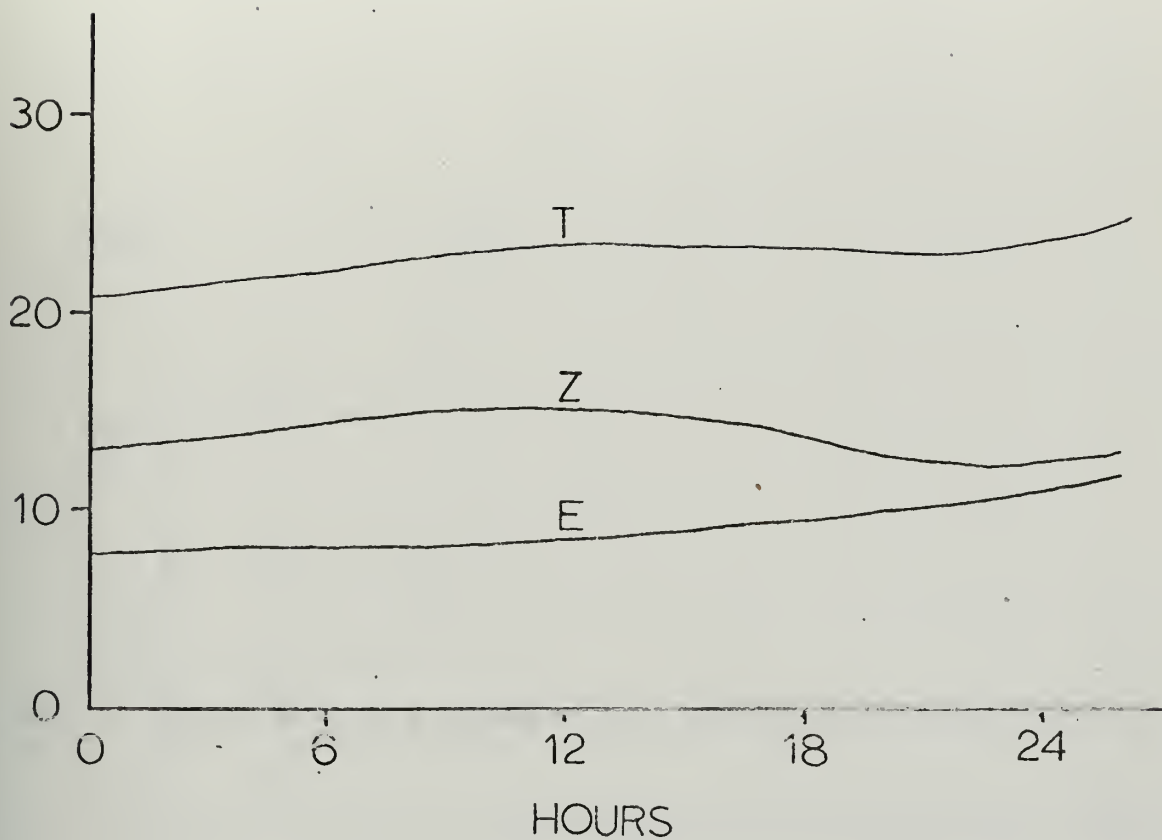


Fig. 10. Total (T), zonal (Z), and eddy (E) kinetic energies vs. time for the barotropic model on the limited grid.



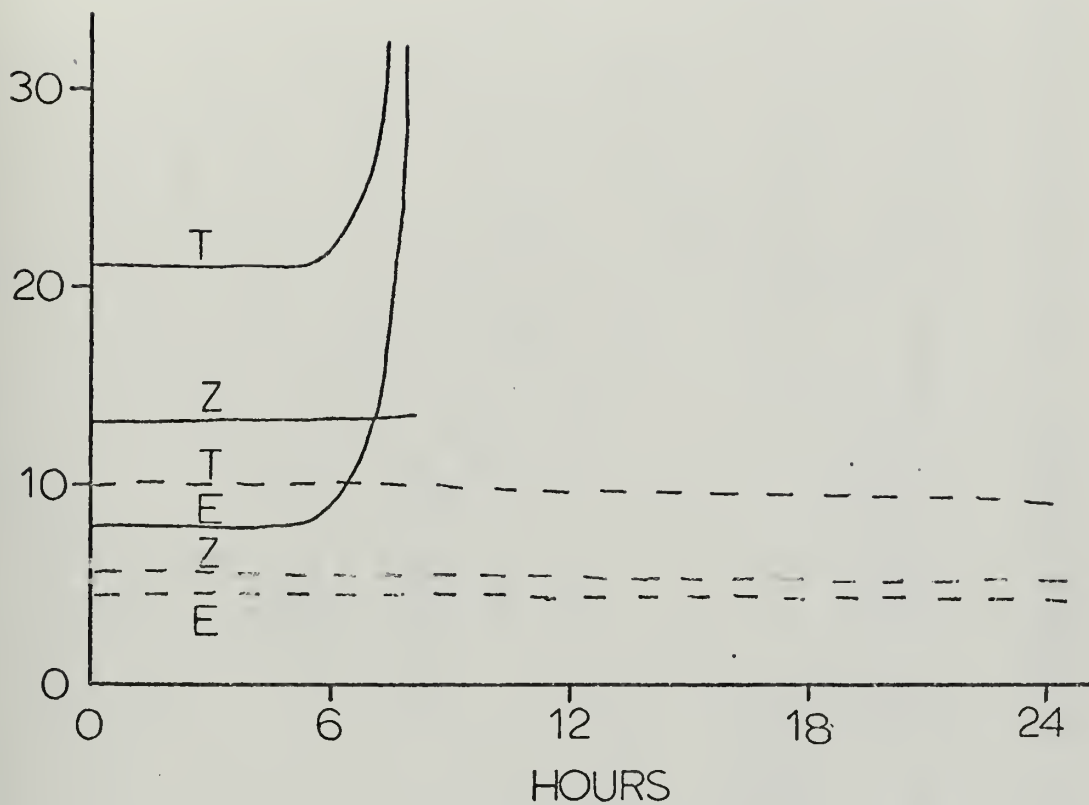


Fig. 11. Total (T), zonal (Z), and eddy (E) kinetic energies vs. time for the two-layer model on the limited grid. Solid lines indicate 250 mb data while dashed lines indicate 450 mb data.



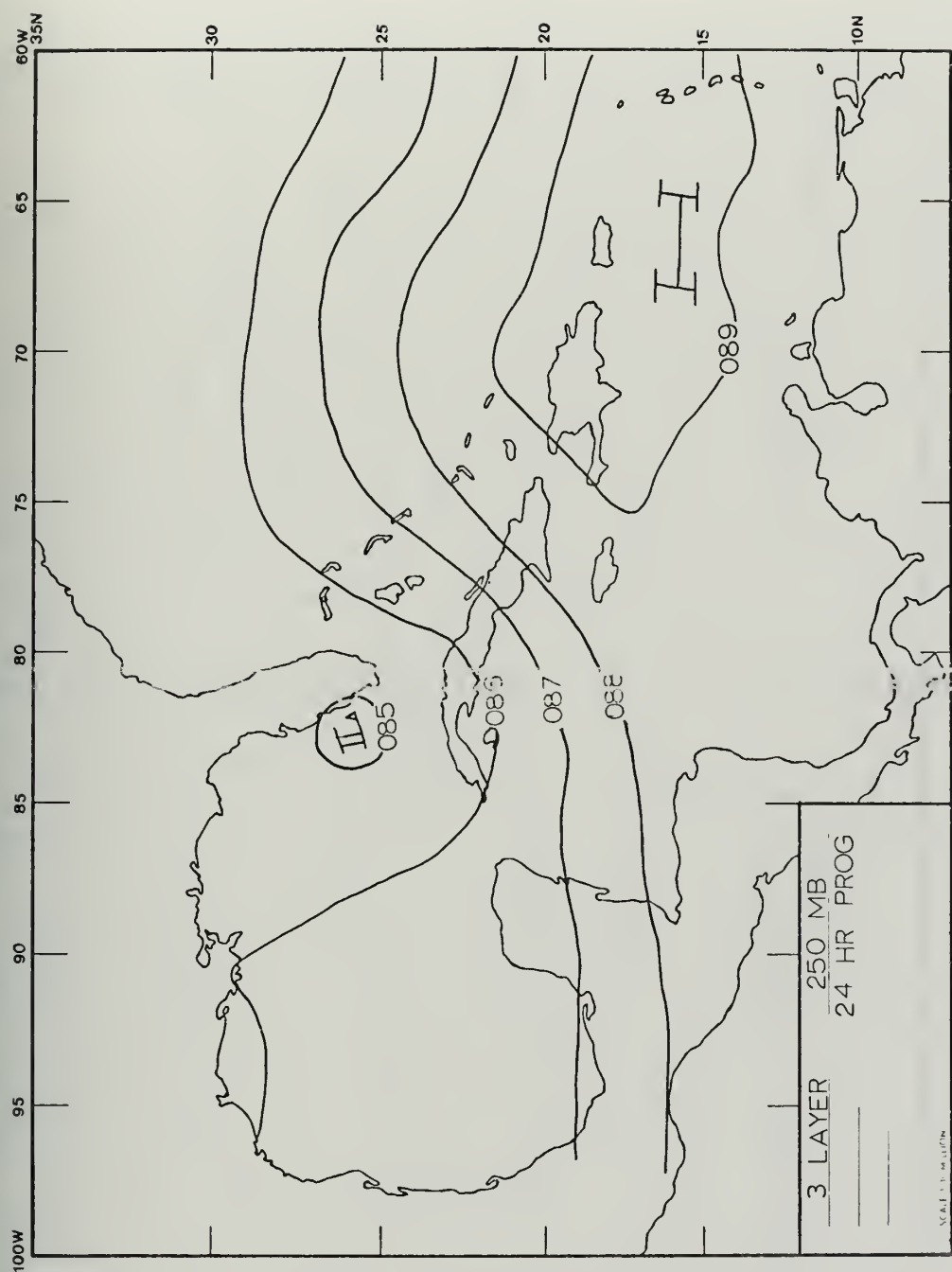


Fig. 12. Twenty-four hour 250 mb height forecast from the three-layer model.



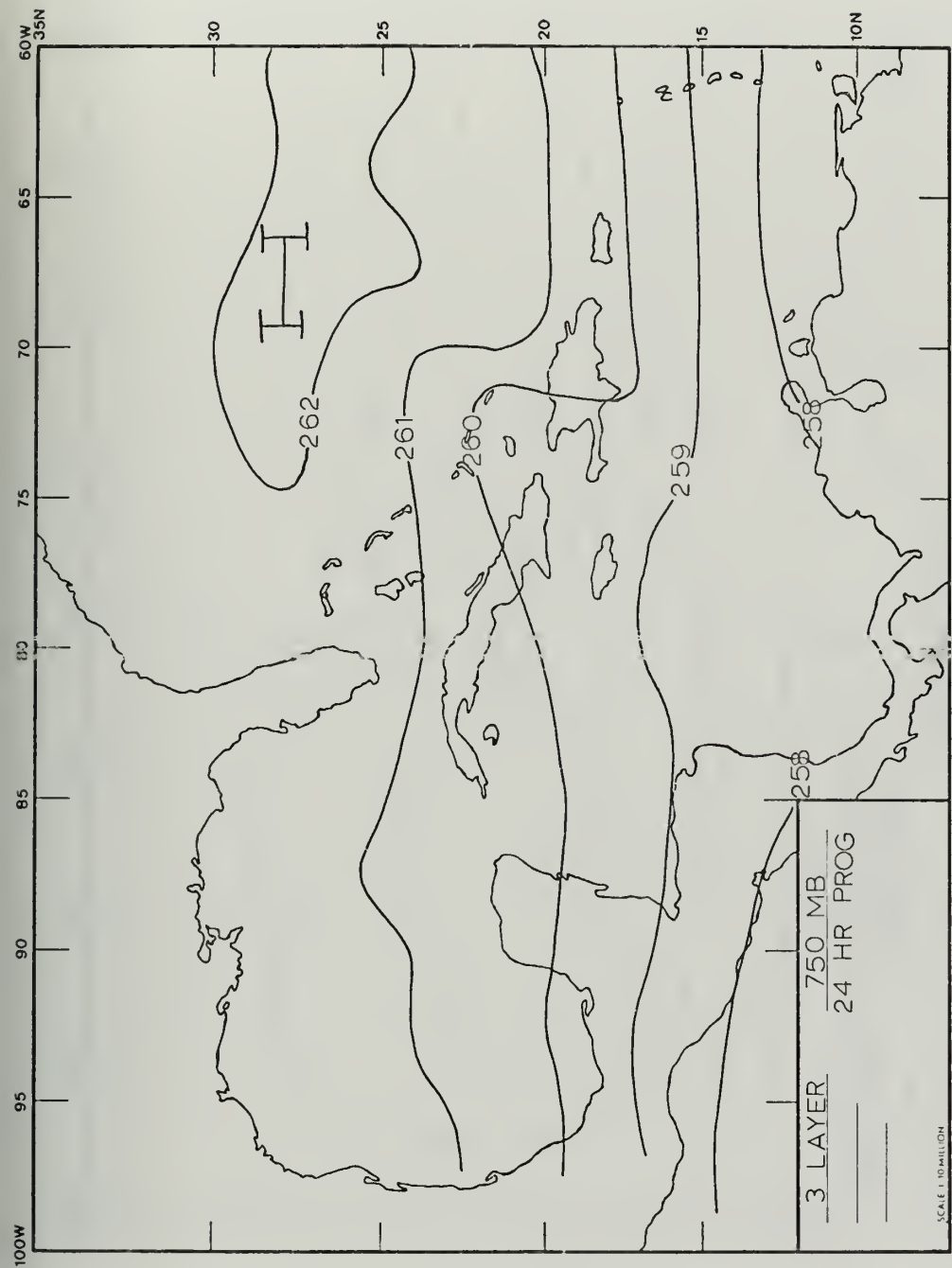


Fig. 13. Twenty-four hour 750 mb height forecast from the three-layer model.





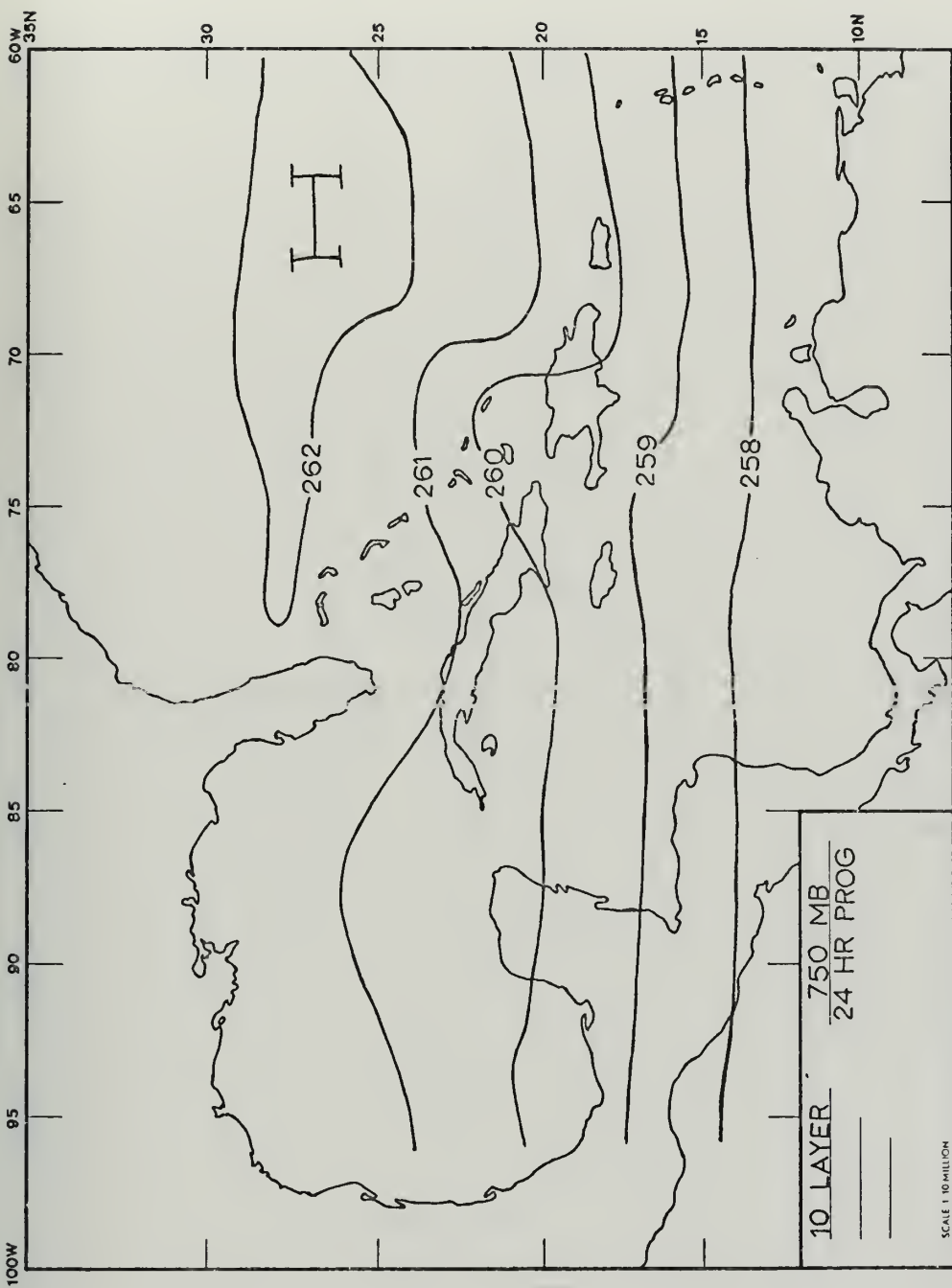


Fig. 14. Twenty-four hour 750 mb height forecast from the ten-layer model.



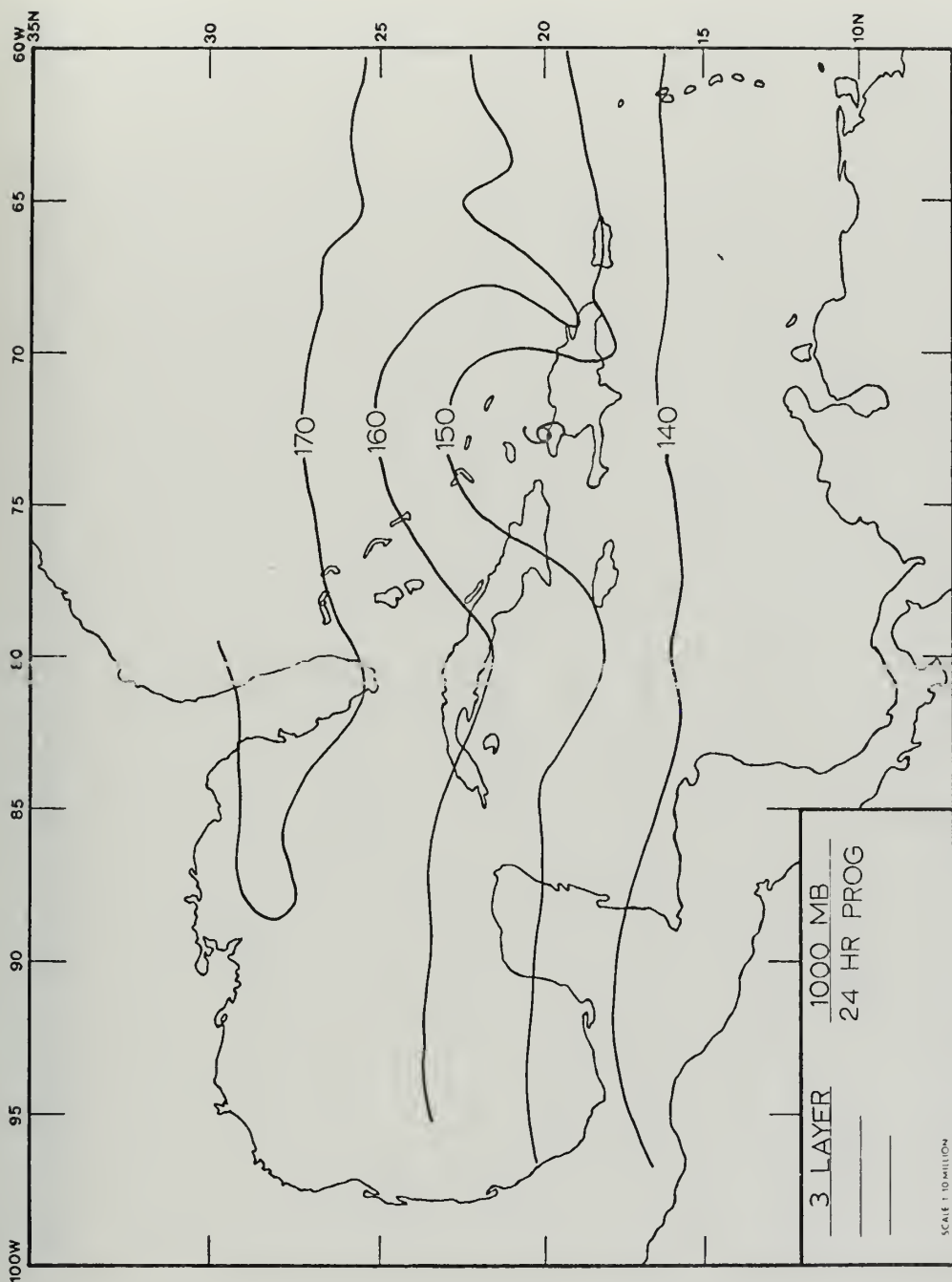


Fig. 15. Twenty-four hour 1000 mb height forecast from the three-layer model.



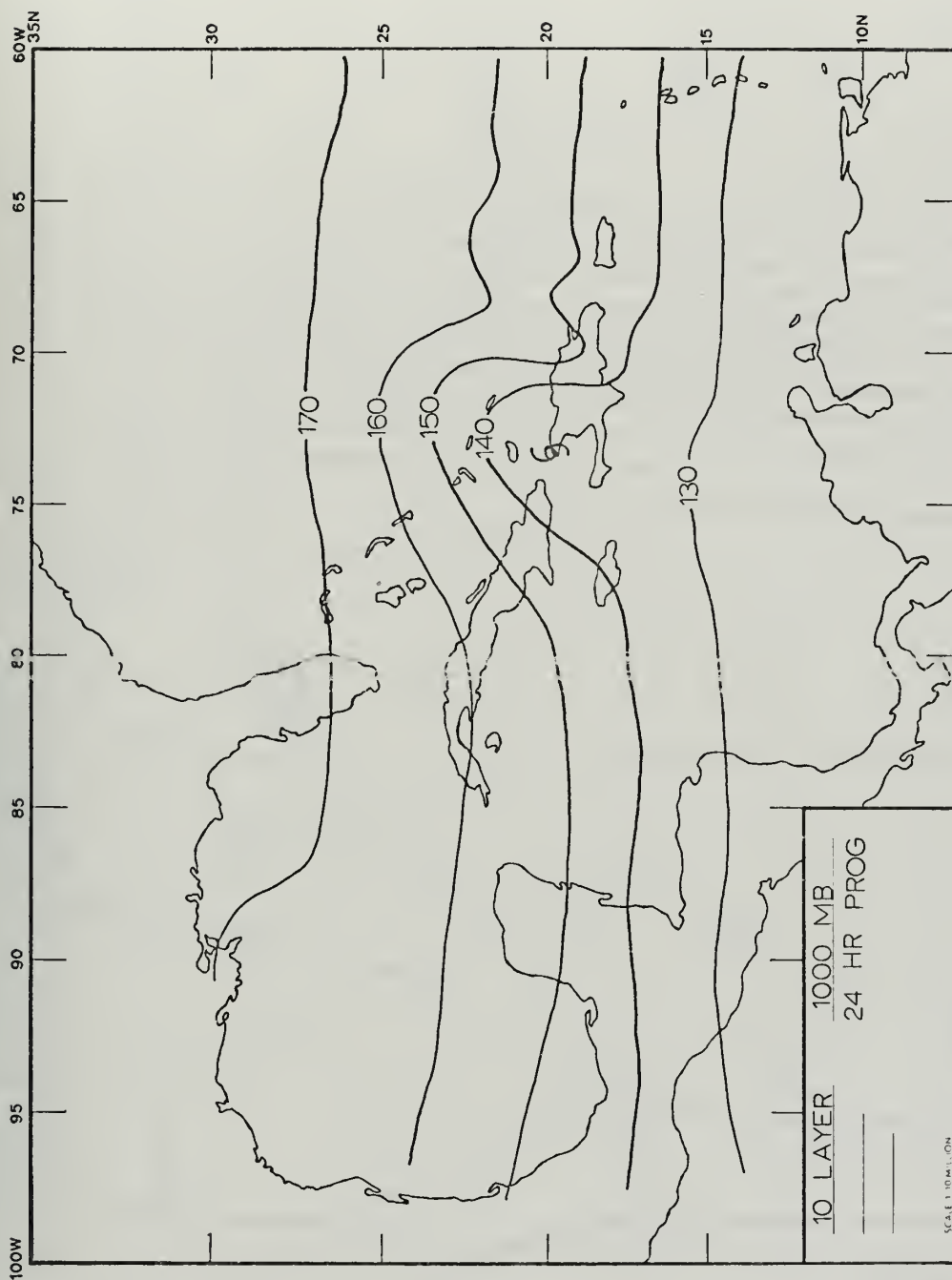


Fig. 16. Twenty-four hour 1000 mb height forecast from the ten-layer model.



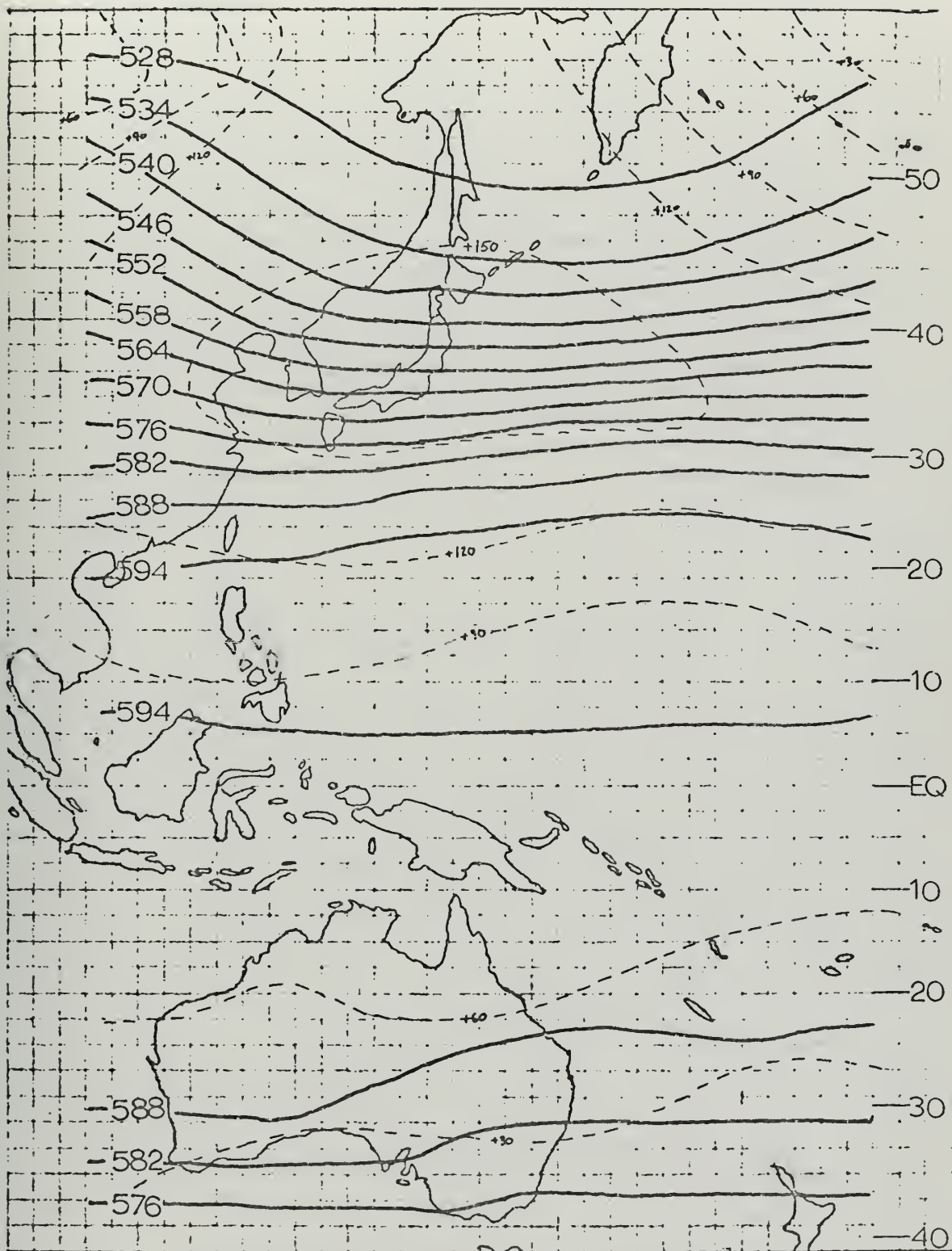


Fig. 17. Initialization of the 500 mb height field by the nonlinear balance equation technique. Solid lines are initial data while dashed lines are the departure from the 500 mb climatology used as input.





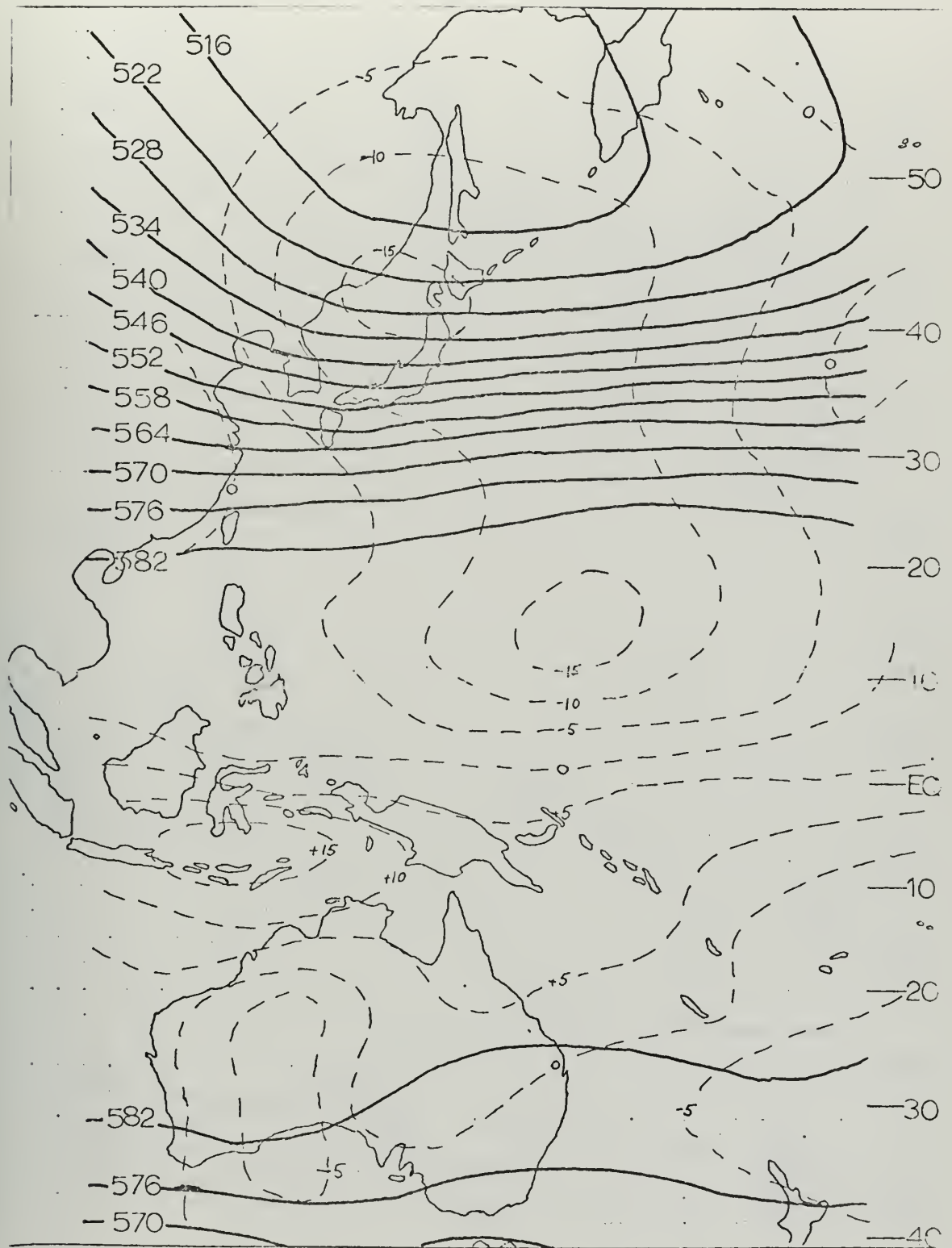


Fig. 18. Initialization of the 500 mb height field by the numerical variational analysis technique. Solid lines are initial data while dashed lines are the departure from the 500 mb climatology used as input.



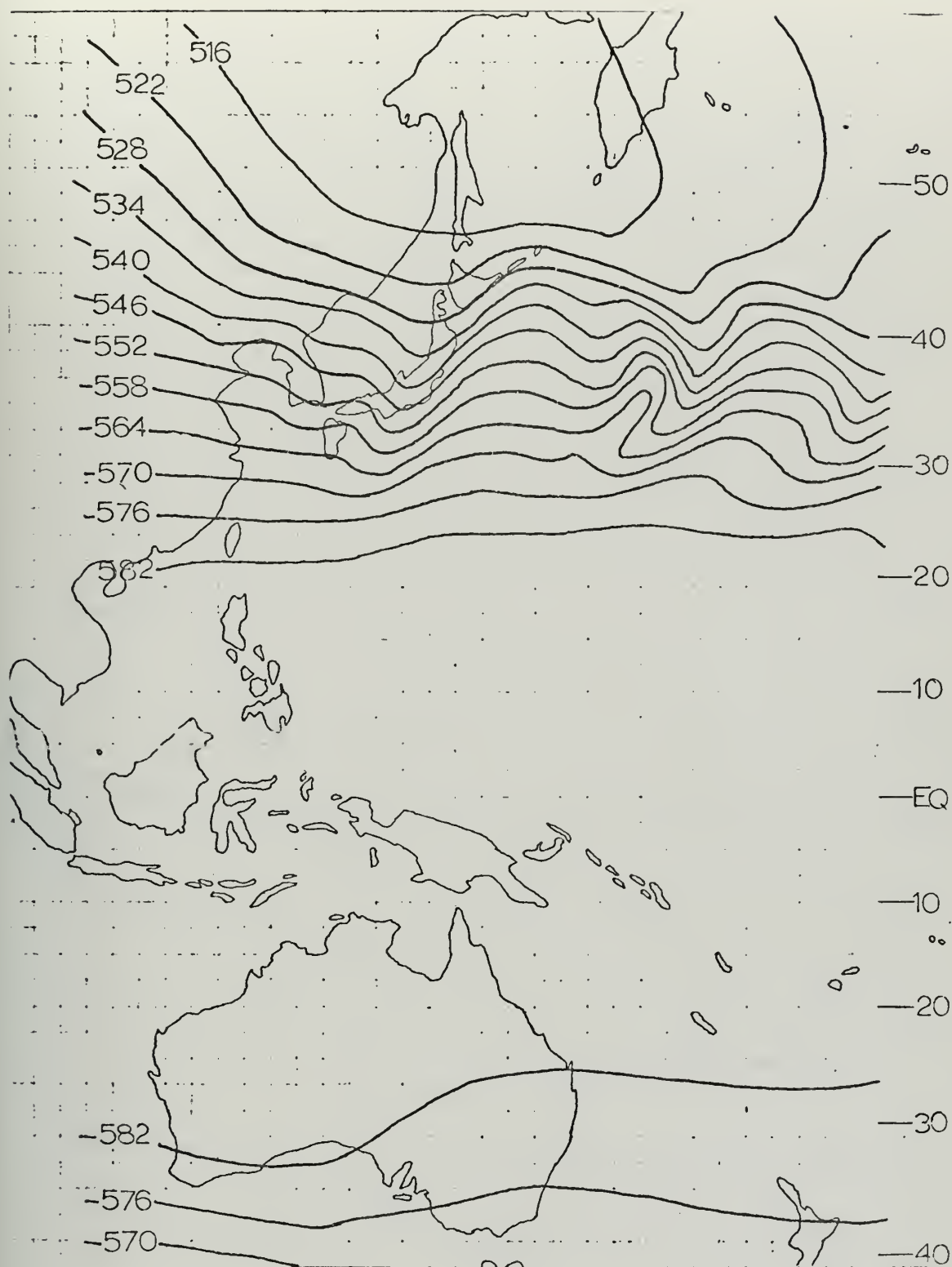


Fig. 19. Twenty-four hour 250 mb height forecast from the barotropic model on the global grid with restoration boundary conditions and numerical variational analysis initialization.



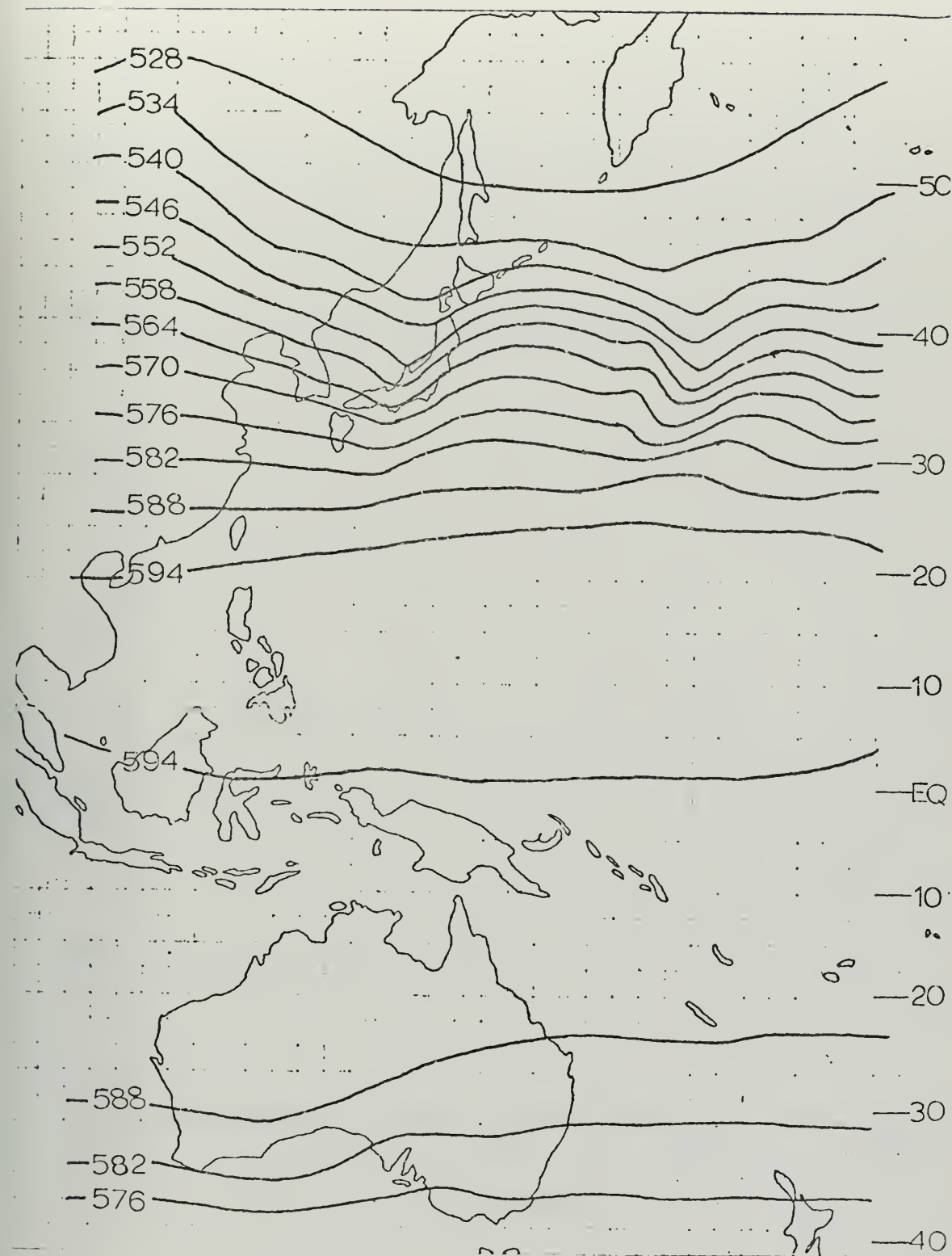


Fig. 20. Twenty-four hour 250 mb height forecast from the barotropic model on the global grid with no-flux boundary conditions and nonlinear balance equation initialization.



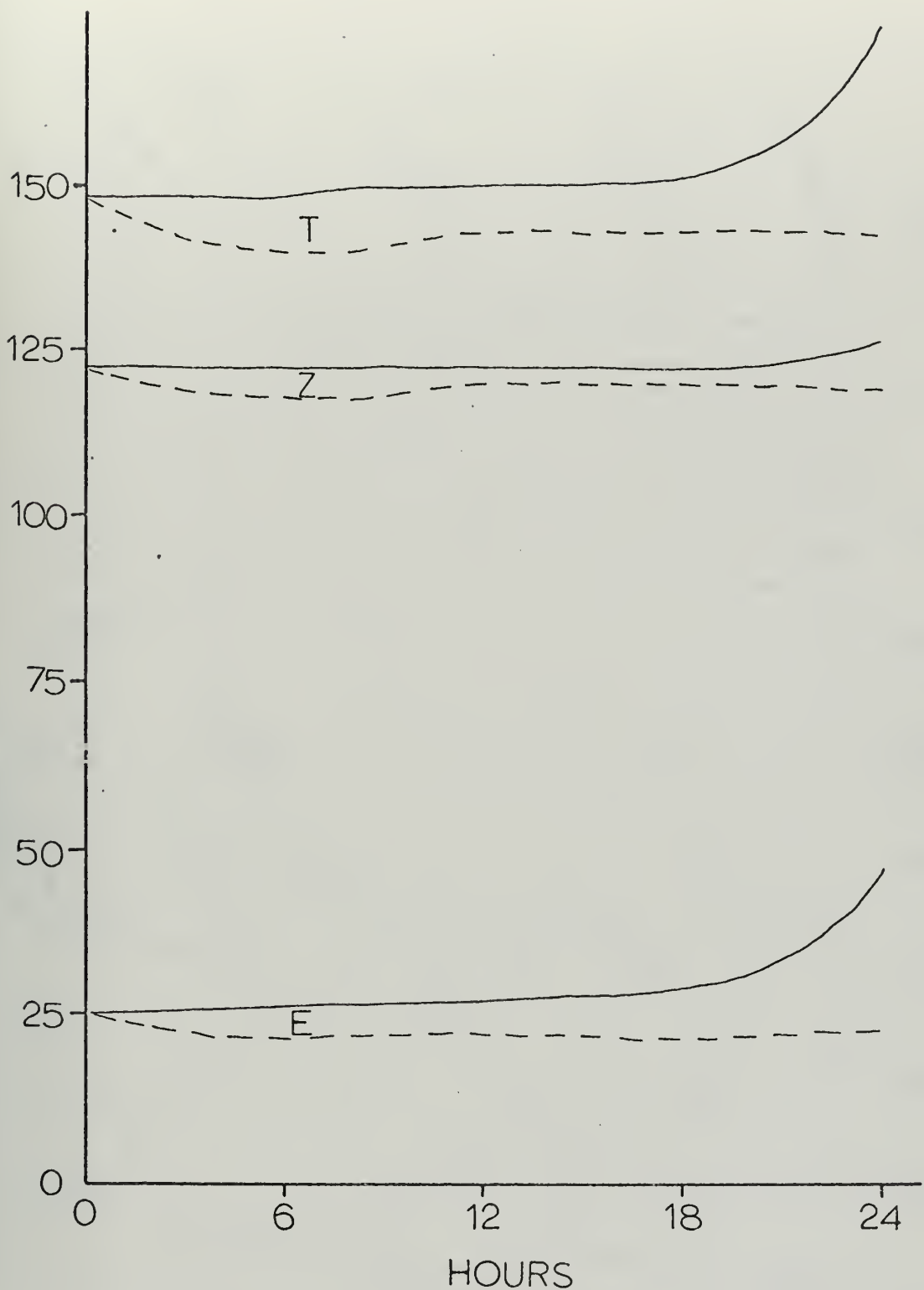


Fig. 21. Total (T), zonal (Z), and eddy (E) kinetic energies vs. time for the barotropic model on the global grid. Solid lines are for the basic model while dashed lines are for the model with diffusion terms included.





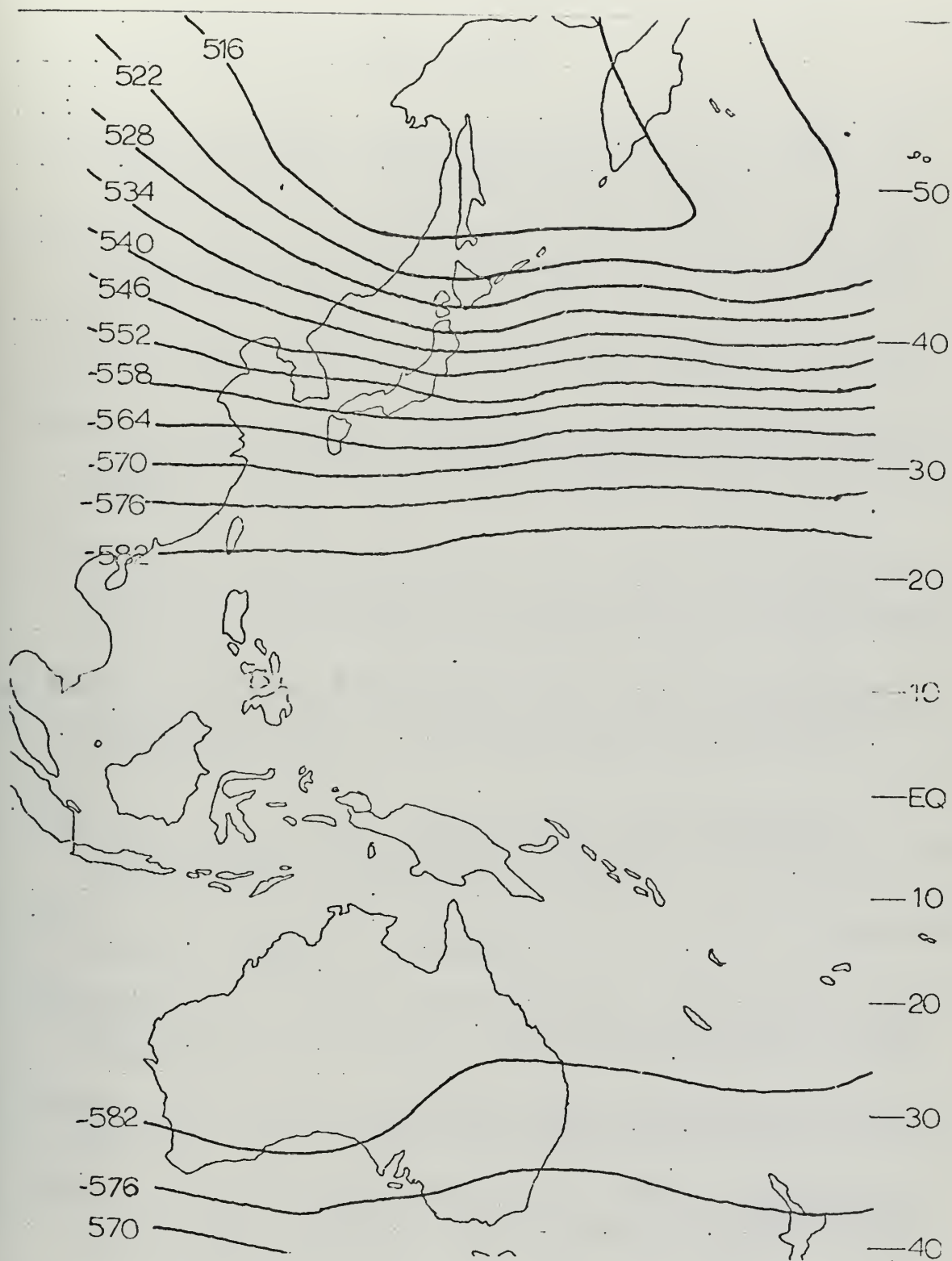


Fig. 22. Twenty-four hour 250 mb height forecast from the barotropic model with diffusion terms, restoration boundary conditions and numerical variational analysis initialization.



## BIBLIOGRAPHY

1. Arakawa, A., 1966: Computational design for long term numerical integration of the equations of fluid motion, Part I. J. Computational Physics, 1, 119-143.
2. Benwell, G.P.R., and Bretherton, F.P., 1968: A pressure oscillation in a ten-level atmospheric model, Quart. J. Roy. Met. Soc., 94, 123-131.
3. Charney, J.G., 1955: The use of the primitive equations of motion in numerical prediction. Tellus, 7, 22-26.
4. Elsberry, R.L., 1969: Preliminary results from diagnostic-prognostic experiments with tropical weather disturbances. Unpublished Interim Report, Naval Postgraduate School.
5. Elsberry, R.L. and Harrison, E.J., 1970: Some primitive-equation model experiments for a limited region of the tropics, Proceedings of the 6th AWS Technical Exchange Conference, U. S. Naval Academy, Technical Report 242.
6. Elsberry, R.L., and Harrison, E.J., 1971: Effects of parameterization of latent heating in a tropical prediction model. To be published in the Monthly Weather Review.
7. Harrison, E.J., 1969: Experiments with a primitive equation model designed for tropical application. M.S. Thesis, Naval Postgraduate School.
8. Hinkelmann, K., 1951: Der mechanisms des meteorologischen larmes. Tellus, 3, 285-296.
9. Hinkelmann, K., 1959: Ein numerisches experiment mit der primitiven gleichungen. C.G. Rossby Memorial Volume, Stockholm.
10. Kesel, P.G., 1968: Experiments with atmospheric equation models. M.S. Thesis, Naval Postgraduate School.
11. Kesel, P.G., and Winninghoff, F.J., 1970: Developing an atmospheric primitive equation model for operational use by the U.S. Navy, Fleet Numerical Weather Central, Monterey Report.
12. Krishnamurti, T.A., 1969: An experiment in numerical prediction in equatorial latitudes, Quart. J. R. Met. Soc., 95, 594-620.



13. Krishnamurti, T.A., 1970: Department of Meteorology, Florida State University, Report No. 70-4, Observational study of tropical upper tropospheric motion field during northern hemisphere summer.
14. Lewis, J.M., 1971: Variational subsynoptic analysis with applications to severe local storms. To be published in the Monthly Weather Review.
15. Miller, B.I., 1969: ESSA Technical Memorandum, ERLTM-NHRL 85, Experiment in forecasting hurricane development with real data.
16. Phillips, N.A., 1960: On the problem of initial data for the primitive equations. Tellus, 12, 121-126.
17. Sasaki, Y., 1958: An objective analysis based on the variational method. J. Met. Soc. Japan, 36, 77-88.
18. Sasaki, Y., 1970: Numerical variational analysis formulated under the constraints as determined by long wave equations and a low pass filter. Monthly Weather Review, 98, 884-898.
19. Schuman, F.G., and Hovermale, J.B., 1968: An operational six-layer primitive equation model. Journal of Applied Meteorology, 7, 527-547.
20. Smagorinsky, J., Manabe, S., and Holloway, L.L., 1965: Numerical results from a nine-level general circulation model of the atmosphere. Monthly Weather Review, 93, 12, 727-768.
21. Vanderman, L.W., and Collins, W.G., 1967: Operational-experimental numerical forecasting for the tropics. Monthly Weather Review, 95, 12, 950-953.
22. Winninghoff, F.J., 1971: Report on global prediction models and initialization. Naval Postgraduate School Report.



# INITIAL DISTRIBUTION LIST

	No. Copies
1. Defense Documentation Center Cameron Station Alexandria, Virginia 22314	2
2. Library, Code 0212 Naval Postgraduate School Monterey, California 93940	2
3. Dr. R. L. Elsberry Department of Meteorology, Code 51Es Naval Postgraduate School Monterey, California 93940	6
4. LCDR Charles G. Steinbruck USS Midway (CVA-41) FPO San Francisco, California 96601	2
5. Dr. R. T. Williams Department of Meteorology, Code 51Wu Naval Postgraduate School Monterey, California 93940	1
6. Dr. R. L. Haney Department of Meteorology, Code 51Hy Naval Postgraduate School Monterey, California 93940	1
7. Dr. J. M. Lewis Fleet Numerical Weather Central Naval Postgraduate School Monterey, California 93940	1
8. Naval Weather Service Command Washington Navy Yard Washington, D. C. 20390	1
9. Commanding Officer Fleet Numerical Weather Central Naval Postgraduate School Monterey, California 93940	1
10. Officer-in-Charge Environmental Prediction Research Facility Naval Postgraduate School Monterey, California 93940	1





11. Department of Meteorology, Code 51  
Naval Postgraduate School  
Monterey, California 93940

1



## DOCUMENT CONTROL DATA - R &amp; D

(Security classification of title, body of abstract and indexing annotation must be entered when the overall report is classified)

ORIGINATING ACTIVITY (Corporate author)

Naval Postgraduate School  
Monterey, California 93940

2a. REPORT SECURITY CLASSIFICATION

Unclassified

2b. GROUP

REPORT TITLE

Some Design Experiments toward an Operational  
Primitive-Equation Model for the Tropics

DESCRIPTIVE NOTES (Type of report and, inclusive dates)

Master's Thesis; September 1971

AUTHOR(S) (First name, middle initial, last name)

Charles George Steinbruck

REPORT DATE

September 1971

7a. TOTAL NO. OF PAGES

55

7b. NO. OF REFS

22

CONTRACT OR GRANT NO.

9a. ORIGINATOR'S REPORT NUMBER(S)

PROJECT NO.

9b. OTHER REPORT NO(S) (Any other numbers that may be assigned  
this report)

DISTRIBUTION STATEMENT

Approved for public release; distribution unlimited.

SUPPLEMENTARY NOTES

12. SPONSORING MILITARY ACTIVITY

Naval Postgraduate School  
Monterey, California 93940

ABSTRACT

A barotropic and two- and three-layer baroclinic primitive equation prediction models are developed from a ten-layer model previously designed for short range forecasts in the tropics. Twenty-four predictions from the models are compared to evaluate any degradation in the forecasts as the vertical resolution of the models decreases. The barotropic primitive equation model on a global tropical grid is used to evaluate the possibility of using a numerical variational analysis as an initialization technique. Initialization of data with the nonlinear balance equation is used as a comparison.



55









Thesis  
S683  
c.1

Steinbruck

Some design experiments toward an operational primitive-equation model for the tropics.

131450

BINDERY

Thesis  
S683  
c.1

Steinbruck

Some design experiments toward an operational primitive-equation model for the tropics.

131450

thesS683

Some design experiments toward an operat



3 2768 002 02253 5

DUDLEY KNOX LIBRARY